

Analysis of Backfill and Pillar Performance in the B-Neath Orebody at the Cannon Mine

D.R. TESARIK*, J.B. SEYMOUR*, and M.E. MUDLIN†

*U.S. Bureau of Mines, Spokane, USA

†Asamer Minerals (U.S.) Inc., Cannon Mine, Wenatchee, USA

U.S. Bureau of Mines researchers and personnel from the Cannon Mine, Wenatchee, WA, USA, installed rock and backfill instruments in the B-Neath orebody to monitor load transfer during primary and secondary mining operations. Conventional rock-mechanics instruments were used in rock pillars and the mine roof, while backfill extensometers were fabricated by the Bureau for use in the cemented primary stopes. Stressmeters and borehole pressure cells placed in secondary rock pillars indicated that stress changes during primary mining in one secondary pillar were approximately seven times the overburden stress. The load-carrying capacity of this pillar was lost before most of the primary stopes had been filled, causing stresses to arch to the abutments. This was verified by very small stress changes in the readings of the backfill instruments.

Two-dimensional, finite-element analyses of the B-Neath orebody predicted failure zones at the same locations as those identified by the rock instruments, but the linear correlation between the relative displacements in the rock and the relative displacements predicted by the numeric model was only 0.24. The model predicted gravity stresses in the backfill, but the statistical correlation was small for the measured and predicted displacements.

This work will further the Bureau's goal of maximizing resource recovery by validating backfill design, evaluating mine stability through the use of numeric techniques, and improving the design of backfill instruments.

Introduction

This study was performed to address the design of cemented backfill for shallow orebodies. The use of cemented backfill in mines in the USA is increasing, and it is important that the effectiveness of backfill from both a scientific and an observational viewpoint should be assessed so that improvements can be made in the designing of future backfills. Specific objectives of this study were to monitor the stress redistribution to cemented backfill and rock pillars during mining, and to evaluate the finite-element method as a tool for the prediction of stress concentrations. Instruments were installed in cemented backfill and rock pillars to record stress and displacement changes as mining progressed.

Fill performance of the B-North orebody, adjacent to the B-Neath, has been analysed by Brechtel *et al.*¹ and Tesarik *et al.*², and the stability of the B-Neath orebody has been evaluated by Brechtel *et al.*³. This additional work in the B-Neath orebody was performed to refine the design of backfill instruments and installation procedures, improve modelling methods, and implement a more thorough instrumentation programme.

Overview of the B-Neath Orebody

The Cannon Mine, located in central Washington, USA, is a joint venture between the operator, Asamer Minerals, Calgary, AT, and Breakwater Resources, Vancouver, BC. A cooperative study between the U.S. Bureau of Mines and Asamer Minerals has focused on the B-Neath orebody (Figure 1), which is a narrow, downward extension of the

B-North orebody. Maximum dimensions are 128 m in thickness, 152 m in length, and 61 m in width. Economic reserves extend from 21 to 192 m above sea level. The northern end of the B-Neath is separated from the B-North and X-stope areas by a shear zone of rock of very poor quality having a thickness of up to 3 m. Both the eastern and western boundaries of the B-Neath have vertical shears up to 30 m thick. The hangingwall consists of weak, interbedded sandstones and sheared claystone³. Shotcrete, described by Baz-Dresch⁴, and resin bolts are used to support these very weak shear zones surrounding the ore. The mine's portal, decline, shaft, and main access drifts are developed in competent rhyodacite porphyry with access to the B-Neath from the east.

Stope Layout and Mining Method

The mining method used is overhand bench-and-fill. Stopes are laid out with an east–west orientation to minimize the effects of the north–south-striking shears. Above the 200 level, levels were driven every 24 m. When additional exploration drilling verified that mining between levels 70 and 200 was economically feasible, levels 70, 110, and 150 were established. The stope widths were initially 9 m, but were reduced to 8 m when poor ground conditions were encountered. Stopes are excavated by the driving of an upper and a lower sill cut 4.6 m high spanning the width of the stope. After these sill cuts are driven the length of the stope, a drop raise and a slot are excavated at the end of the stope to connect the two levels. The resulting stope block is then benched towards the access drift on the upper level while blasted ore is removed on the lower level (Figure 2).

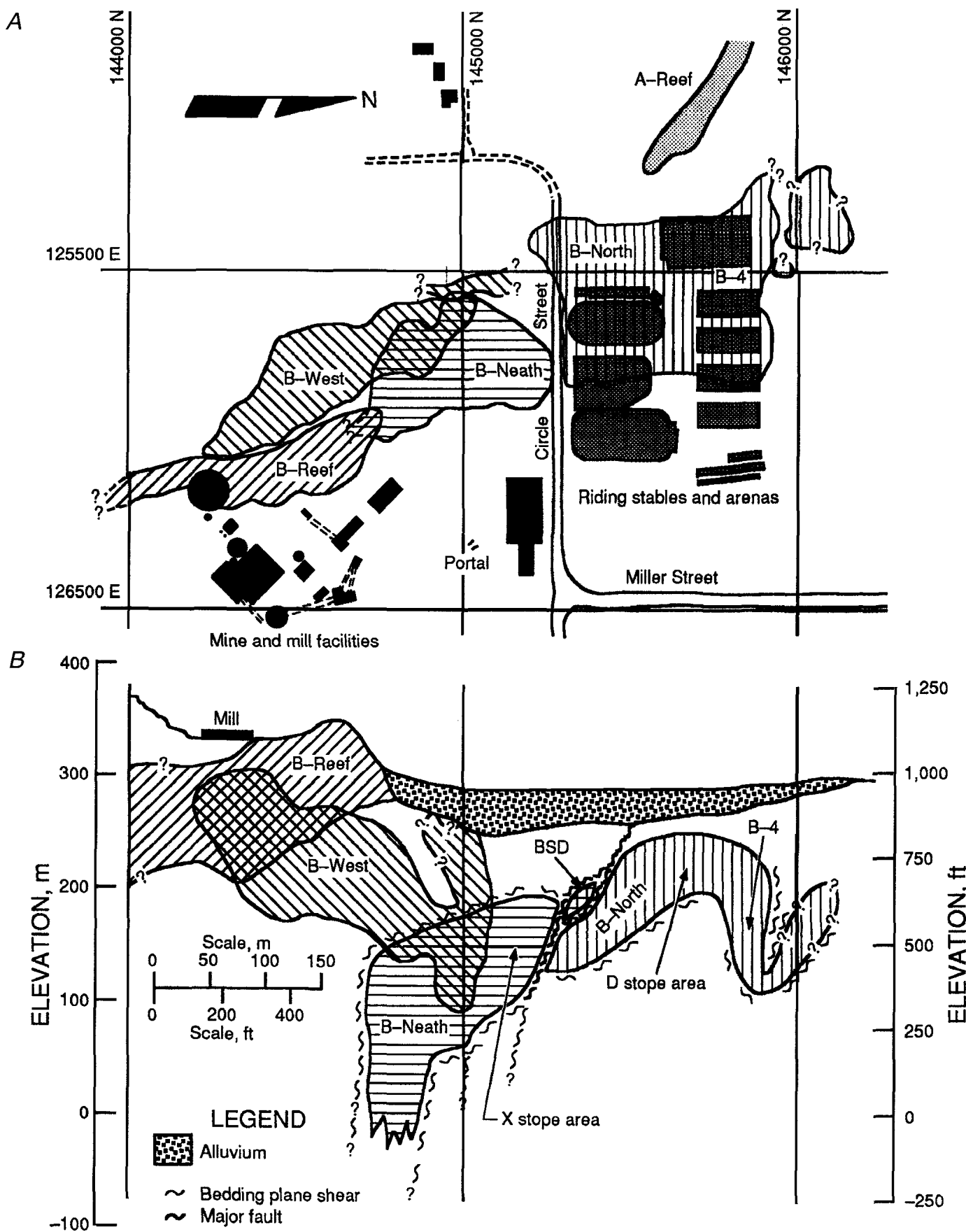


Figure 1. B-Reef ore zone: A, Plan view; B, Cross-section looking southwest (courtesy of Cannon Mine)

Load-haul-dump (LHD) units load the blasted ore onto 24 Mt diesel trucks, which haul the ore to the main ore pass on the 550 or 600 levels.

Cemented fill is dumped into the open stope from the upper heading after the stope block has been benched. When ground conditions are good, the stope is filled completely but, in cases where shears increase the risk of localized pillar failure, the pillar is benched and filled in several steps along its longitudinal axis. The backfilled level then serves as the mucking level for the next vertical stope interval. The sequence is repeated until the top of the ore block is reached. Cemented fill is then pushed tightly to the hangingwall by use of a 1,2 m² plate mounted on a beam of an LHD.

After the mining and backfilling of the primary stopes, secondary pillars are extracted in a similar way and are filled with waste rock. However, cemented fill has been dumped into the stopes between the 200 and 280 levels to construct a competent back for subsequent mining between levels 150 and 200 (Figure 3).

Placement of Instruments

Cemented backfill pillars X80, X86, X92, X97, and X04 were instrumented with embedment strain gauges, earth pressure cells, and horizontal and vertical extensometers. These instruments were placed on several levels in the centre of the north-south cross-section of the orebody in anticipation of load transfer during the secondary pillar extraction, as shown in Figure 3. When the mining schedule permitted, a cluster of all four types of backfill instruments was installed. This technique ensured that some data would be collected at each station and would provide duplicate information when all the instruments functioned. The backs in primary pillars X80 280 (280 refers to elevation in feet above sea level and also denotes the mine level) and X86 280 were monitored with borehole

extensometers angled from adjacent secondary pillars X83 and X89, respectively. Secondary rock pillars were instrumented with uniaxial stressmeters, borehole pressure cells, and horizontal and vertical borehole extensometers (Figure 4).

Placement of the instruments in the backfill and secondary pillars was designed so that the redistribution of stresses during mining could be tracked. For example, a stress increase in the readings of the backfill instruments would be expected when a stress decrease was indicated by the rock instruments. Also, vertical borehole extensometers were placed in the rock above the top sill cut of stopes X80 and X86 to work in conjunction with earth pressure cells placed beneath them in cemented backfill. Compressive stress recorded by an earth pressure cell combined with a decrease in strain rate recorded by an extensometer could indicate when the backfill started to load.

All the transducers in the instruments were vibrating wire, except for the vertical borehole extensometer in X89 400, which was based on resistance. The use of vibrating-wire technology proved useful in that cables cut by blasts or machinery were quickly repaired with splice connectors without the necessity of recalibrating the transducer.

Design of the Instruments

Custom-designed horizontal extensometers were used in the B-Neath orebody to measure lateral dilation and contraction in the cemented backfill. The measurement rod was constructed of steel pipe with a bearing plate at one end. The bearing plate was placed approximately 1 m from the rib, and the other end was supported at a slip joint in a steel box in the centre of the stope. Both the northern and southern halves of the stope had measurement rods. Compression fittings were used to secure the transducer heads to the steel box, and the threaded ends of the transducers were screwed into plugs in the steel pipes.

Vertical extensometers were installed in BX-sized diamond-drill holes in the cemented backfill from the upper sill cut. Polyvinyl chloride (PVC) pipe was inserted inside the drill steel to keep the hole open after the steel had been removed. Steel rebar welded to steel rod of 1,6 cm diameter served as the downhole anchor. Sections of steel rod approximately 1,5 m long coupled together to form the extensometer rod were inserted in the PVC pipe and lowered down the hole. A mixture of cement and water was poured into the hole to secure the rebar anchor, and the PVC pipe was removed. Dry sand was then poured down the hole to prevent pieces of backfill from spalling and wedging between the steel rod and the backfill wall. The head assembly, which consisted of the displacement transducer and bearing plate, was placed over the steel rod, and the transducer was screwed into the rod. Finally, the protective head was bolted onto the bearing plate.

The backfill instruments were installed approximately 1,5 m below the final grade of the stope backfill to ensure proper cable protection. The cables were strung from the instruments to the upper stope access drift, and both the cables and the instruments were then covered with cemented backfill. Because the top of the cemented backfill in this stope served as the mucking level for the next lift in the stope column, the signal cables were not recovered until mucking and backfilling had been completed on the next lift.

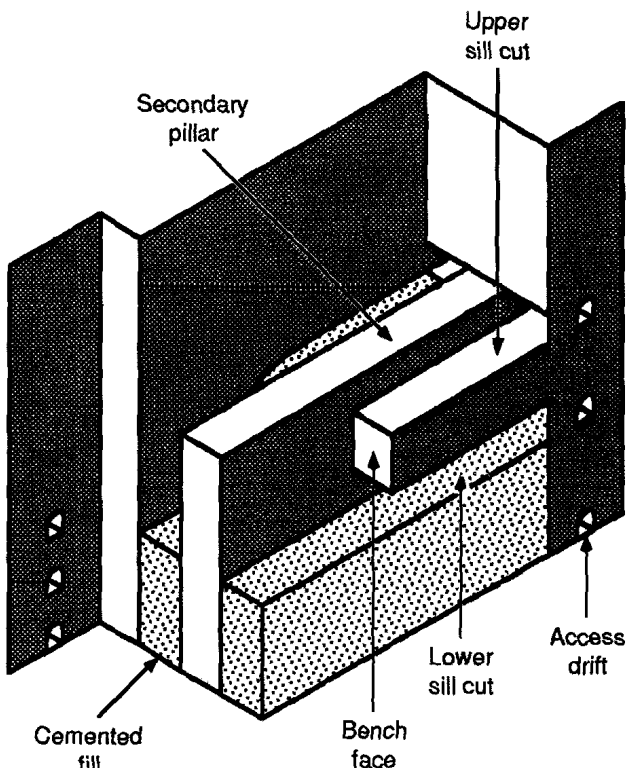


Figure 2. Schematic diagram showing the mining method

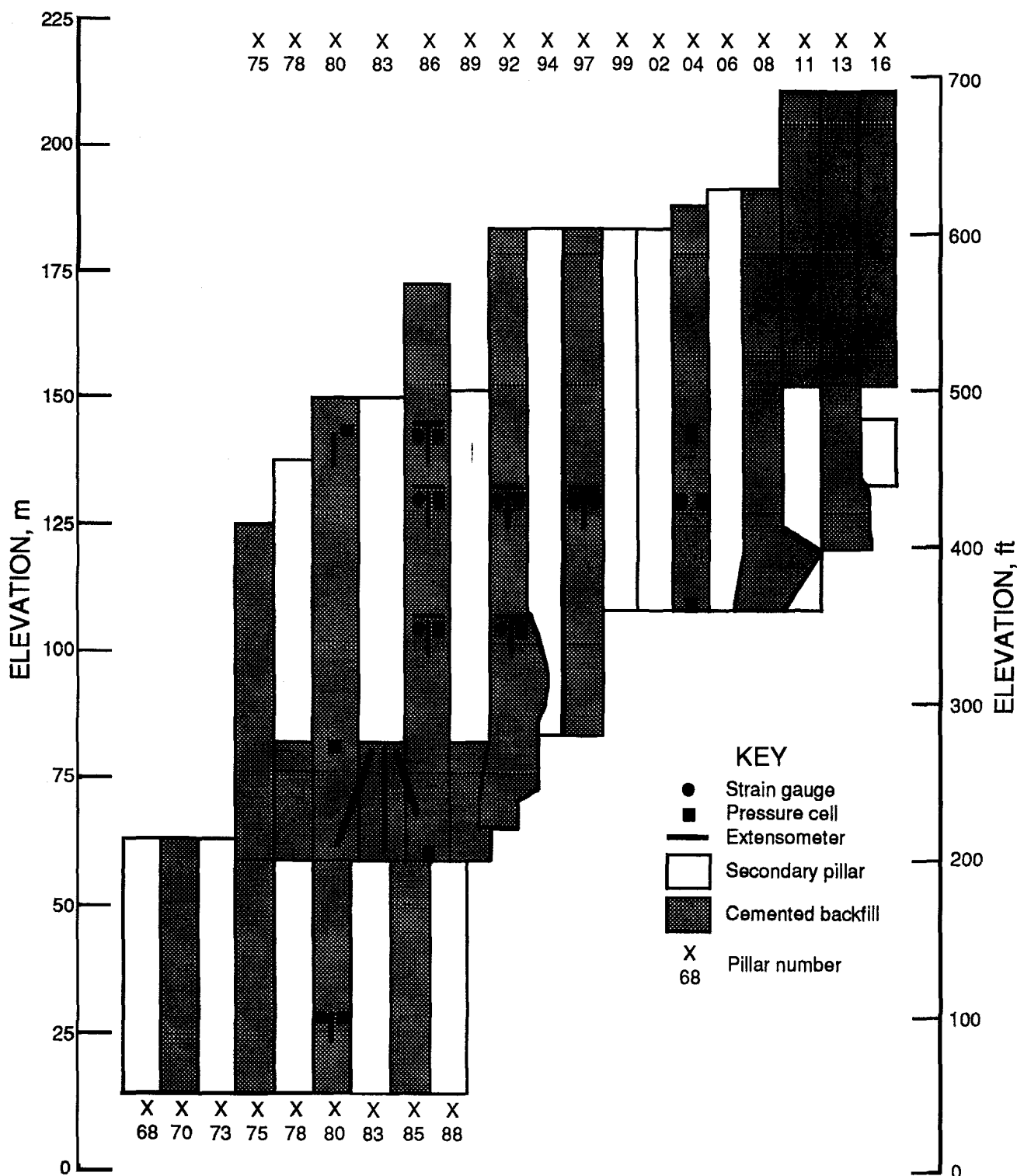


Figure 3. Placement of the backfill instruments

Rock Instrumentation Results

The horizontal extensometers and uniaxial stressmeters located in the secondary pillars indicated that there were areas of localized failure or slabbing in these pillars. The decreases in stresses recorded by four uniaxial stressmeters in X83 280 ranged from 0,27 to 4,9 MPa in a 7-day period after the X80 200 and X86 200 headings had been completed and excavation of the X80 bench from the 200 to 280 level was in progress. Although the range in stress change among these instruments was large, the direction of change indicated that there was a failure zone at this location. Similarly, one of the stressmeters located at

X83 360 recorded a change in stress of approximately 17,5 MPa between days 365 and 384, as well as a tensional relative displacement of 4,8 mm in a horizontal extensometer after the X80 360 bench and the X86 360 heading had been completed (Figures 5 and 6). The stress associated with this displacement was approximately 15 MPa when the laboratory modulus of deformation was used. This value exceeded the estimated strength of the silicified sandstone in tension, and suggested that the rock had failed in tension. Days 365 and 384 refer to the number of days after 25th May, 1988, the starting date for all the plots.

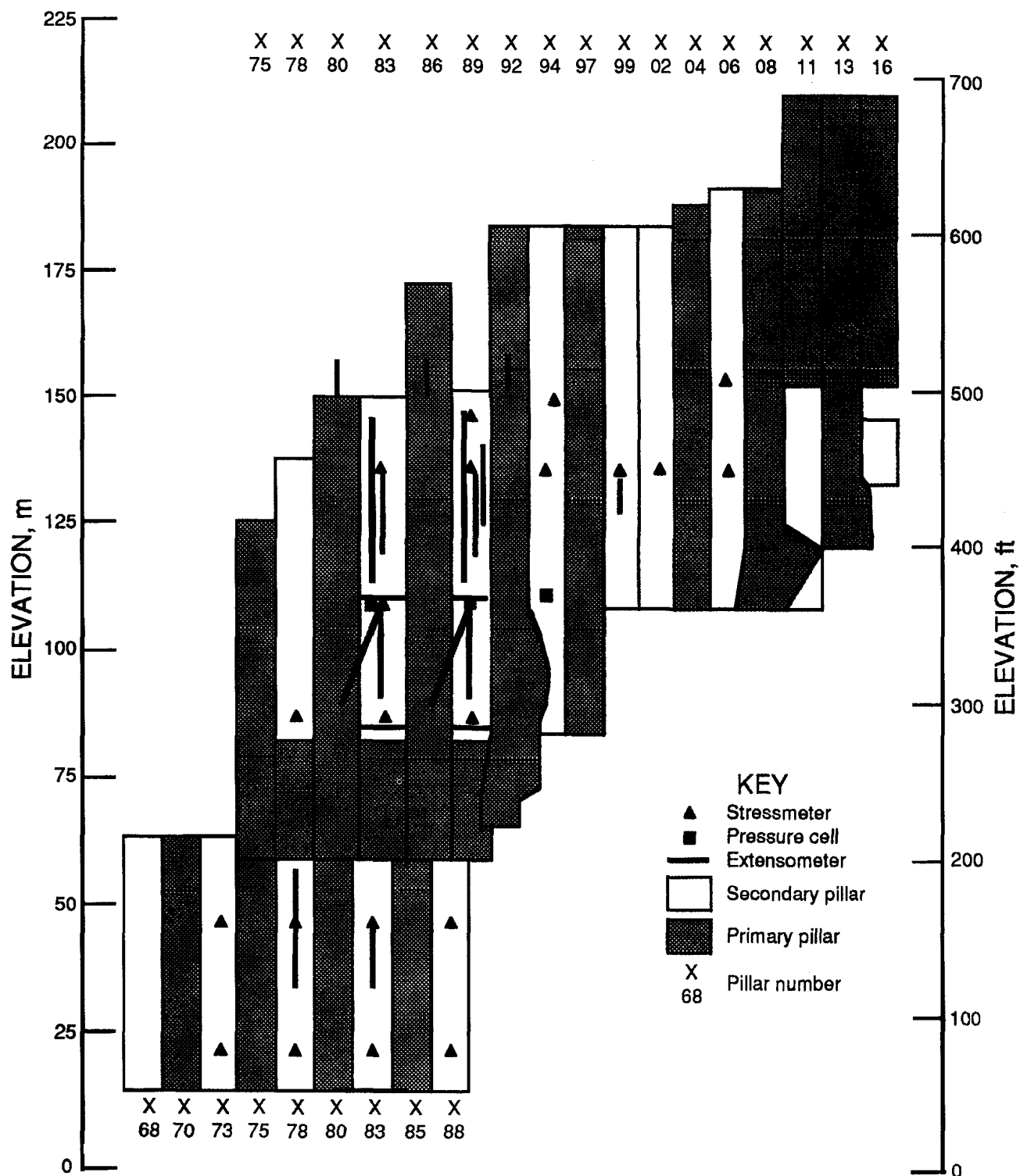


Figure 4. Placement of the rock instruments

The changes in compressive stress measured during primary mining by the wedge-style uniaxial stressmeters and borehole pressure cells showed that more load was transferred to secondary rock pillar X99 than to the other secondary pillars. The average stress change in X99 was -22.7 MPa; the next highest average stress change was -2.6 MPa in X83. The plot of stress changes recorded by one of the stressmeters in X99 is shown in Figure 7. If all the secondary pillars had carried overburden load, the expected stress change at the 440 level would have been approximately -3.7 MPa. The small values and stress decreases recorded by the stressmeters indicated that localized failures had occurred in the secondary pillars.

The vertical extensometers placed in the roof of the access drift aligned with pillars X80, X86, and X92 at the 480 level indicated that the mine back remained stable at this level, with maximum microstrains of 56, 450, and 200, respectively. The extensometer next to X86 responded to the mining of the X80 480 heading with changes in microstrain of 237 and 137 for the short and long anchors, respectively. The changes in the other two instruments did not appear to correspond to specific mining events.

The borehole extensometers installed in X83 360 and X89 360 were useful for monitoring the safety of the back at the 280 level in adjacent pillars. Although the strain in X86 possibly exceeded the elastic range of the rock, the flat

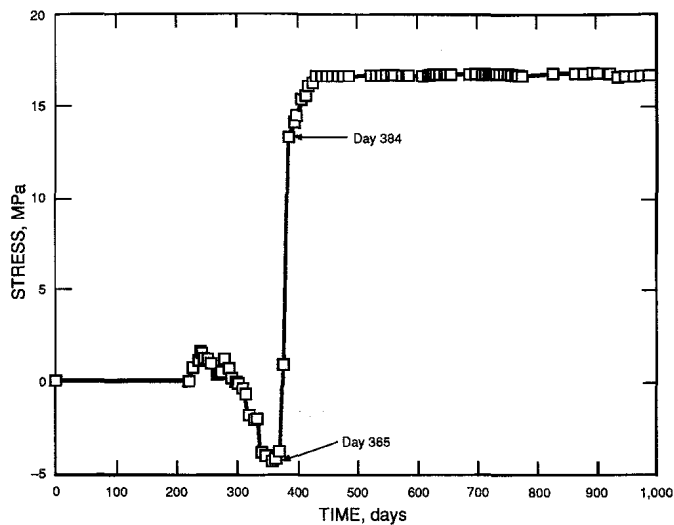


Figure 5. Plot showing stress changes recorded by the stressmeter in X83 360

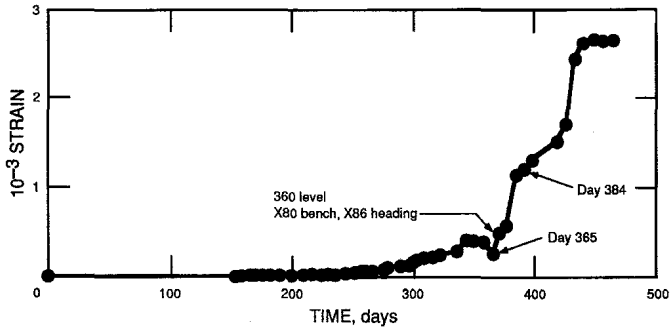


Figure 6. Plot showing the strains recorded by the horizontal extensometer in X83 360

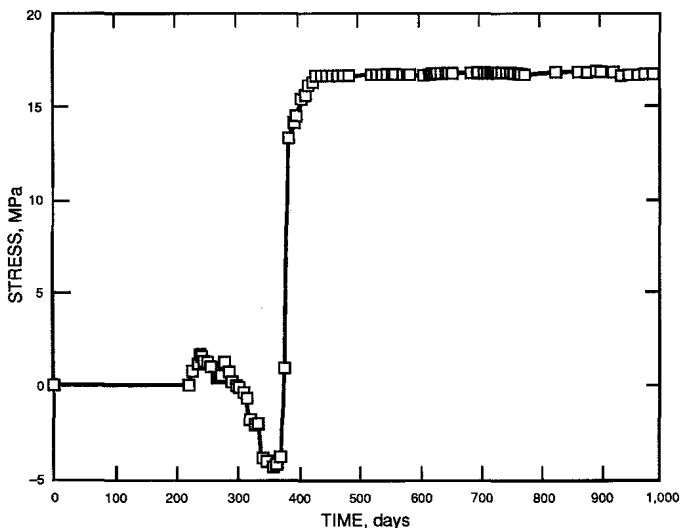


Figure 7. Plot showing the stress changes recorded by the vertical stressmeter at X99 440

slope of the 18,6 m gauge indicated that the back remained competent (Figure 8). The 19,2 m gauge did not function after day 309.

Backfill Instrumentation Results

The maximum compressive measurements from the earth pressure cells were compared with the measurements from

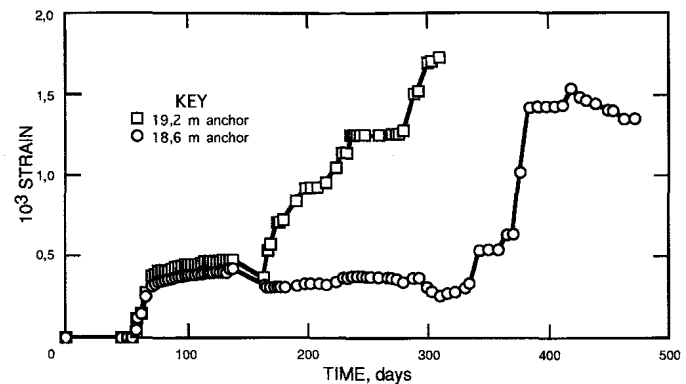


Figure 8. Plot showing strains recorded by the borehole extensometer (the borehole containing the instrument dips -60° from X89 360 to X86 280)

the vertical backfill extensometers and embedment strain gauges by the use of Hooke's law for uniaxial loading in the vertical direction. A value of 689,4 MPa was used as the modulus of the backfill. This value is based on stress-strain relations produced from instruments located in cemented backfill in the B-North orebody. So that the measured values could be compared with stresses caused only by the weight of backfill over the instrument, stresses were also calculated with 2114,4 kg/m³ as the unit weight of the backfill. As shown in Table I, the measured compressive stresses were less in most cases than those that were calculated, indicating that the cemented-backfill pillars did

Table I
Maximum compressive stresses in cemented backfill

Stop level	Instrument*	Maximum measured stress, MPa	Calculated stress, MPa
X80 110	VFX	0,00	-2,50
	ESG	-0,28	-2,50
	EPC	0,00	-2,50
X80 280	EPC	-0,69	-1,42
	VFX	-0,69	-0,13
	EPC	-0,69	-0,13
X83 280 to X83 200	VFX	0,00	-1,42
	VFX	0,00	-1,42
	VFX	0,00	-1,42
X86 200	EPC	0,00	-2,37
	VFX	-0,28	-1,36
	ESG	-0,01	-1,36
X86 440	EPC	-0,34	-1,36
	VFX	0,00	-0,85
	ESG	-0,03	-0,85
X86 500	VFX	-0,17	-0,13
	ESG	-0,21	-0,13
	EPC	0,00	-0,13
X92 360	VFX	-1,03	-1,58
	ESG	-0,33	-1,58
	EPC	0,00	-1,58
X92 440	VFX	-0,28	-1,07
	ESG	-0,41	-1,07
	EPC	0,00	-1,07
X97 440	VFX	-0,10	-1,07
	ESG	-0,24	-1,07
	EPC	-0,19	-1,07
X04 360	EPC	-0,17	-1,67
	EPC	-0,69	-0,79
X16 590	EPC	-1,38	-0,66

VFX = Vertical fill extensometer

ESG = Embedment strain gauge

EPC = Earth pressure cell

not carry any redistributed stresses. A possible explanation for the consistently small stresses in the backfill is that, once the first backfill lift had cured, the additional weight applied by subsequent lifts could be carried in shear at the interface between the rock and the cured backfill.

All three extensometers installed in the cemented backfill from X83 280 to measure displacements during the undercutting operations in the lower levels of the B-Neath registered from 154 to 211 microstrain in tension. These data reflect the mining of X80 from the 70 to the 150 levels. More displacement is expected as mining in this area proceeds.

The horizontal extensometers recorded a compressive trend from 73 to 145 days after installation, followed by a relatively small change in strain rate that varied in direction depending on time and instrument location. This result was also observed in the B-North ore zone, but the reason is not known.

Numeric Modelling

The finite-element program used to model the north-south cross-section of the mine was UTAH2⁵. An elastic, perfectly plastic model was used for all materials. The yield criterion used was the Drucker-Prager, where strength depends on all three principal stresses, and associated flow rules were applied in the determination of strains in the yielded elements. The ANSYS⁶ preprocessor was used to define the mine geometry and automatically mesh the cross-section, while the post-processor was used to analyse the failure zones graphically.

The finite-element mesh included both the B-North and the B-Neath orebodies, with the top of the mesh representing the ground surface. The other mesh boundaries were approximately 360 m from the shear zone surrounding the orebodies. Because the stresses in the elements located at the mesh boundaries did not change when the excavations were modelled, this distance was sufficient to eliminate the effects of boundary conditions on the numeric results. The primary stopes in the B-Neath orebody were meshed with a column in which the elements were 0,30 m wide and 1,5 m high along the vertical interface with adjacent pillars. When cemented backfill was placed in the stope by the model, these elements were given a shear strength of zero to eliminate the effects of high-modulus rock on the backfill elements. If an interface element is not used, the modelled stresses in the backfill are erroneously lower than the stresses caused by the weight of the overlying material².

The remaining elements in the B-Neath orebody were approximately 1,5 m on each side, grading into larger elements as the distance from the orebody increased. The average width and height of the elements for the B-North orebody were approximately 6,4 m. Small elements were not necessary because the purpose in the modelling of the B-North orebody was to provide realistic pre-mining loading conditions for the B-Neath.

The mining sequence modelled by UTAH2 was the same as the actual mining and filling of the B-Neath; however, the plane strain model could not account for activity along the longitudinal axes of the pillars. Excavation or filling in the model was based on the completion date of the activity in the mine. Because the stopes in the B-North were oriented north-south, the mining of this orebody was simulated in the model by mining and filling lifts of 15 m from the footwall to the hangingwall. Forty cuts and thirty filling steps were used to model the excavation and filling

of the B-North, the primary pillars in the B-Neath above the 200 level, the secondary pillars from the 200 to 360 levels in the B-Neath, and X80 from the 70 to the 110 levels. Additional mining was not modelled because neither the instruments nor the numeric results indicated significant loading of the backfill.

Laboratory material properties used in the computer model are listed in Table II. The properties of the silicified sandstone, unsilicified sandstone, and cemented backfill were obtained from unpublished reports submitted to Asamera Minerals (U.S.), Inc., by J. F. T. Agapito and Associates, Inc. Because the reported values for mudstone⁷ exceeded the laboratory values for unsilicified sandstone and field observations indicated that the sheared mudstone was very weak, the mudstone's material properties were set to one-half those of the unsilicified sandstone. Both the andesite and the rhyodacite intrusions were given the material properties of basalt⁸. The properties of the uncemented fill and overburden were obtained from one-dimensional compression tests on mine backfills⁹ and textbook values for soils¹⁰, respectively. Pre-mining stresses were initialized with 2306 kg/m³ as the unit weight of the material to be consistent with the overcoring results³. The cemented and uncemented backfill had unit weights of 2402 kg/m³ and 2114 kg/m³, respectively.

Table II
Laboratory properties used in the numeric analysis

Material	Property*, MPa			ν^{\dagger}
	E	C	I	
Silicified sandstone	12 960	45,6	4,6	0,25
Unsilicified sandstone	11 722	25,4	2,5	0,25
Andesite/rhyodacite	59 388	251,6	25,2	0,31
Mudstone	5 861	12,7	1,3	0,25
Cemented fill	3 792	8,3	2,1	0,30
Uncemented fill	159	4,1	1,0	0,30
Overburden	19	0,7	0,03	0,30

* E = Modulus of deformation

C = Unconfined compressive strength

I = Tensile strength

ν^{\dagger} = Poisson's ratio

Figure 9 shows the measured versus the predicted relative displacements for the borehole extensometers placed in rock. The linear correlation coefficient for these 81 pairs is 0,24. The eight largest measured positive displacements can be considered to be outliers because they were recorded by instruments located in plastic zones identified by the finite-element code, and because the magnitude of the measured displacements was much greater than the magnitude of the predicted displacements. Without these eight points, the correlation coefficient becomes 0,58, with the measured relative displacements approximately three times the value of the predicted displacements. Possible reasons for this low correlation are that the two-dimensional cross-section did not adequately represent the three-dimensional orebody; that the stress redistribution was dependent on complex geology that was not modelled; and that the mining activity in the B-West, not accounted for in the model, caused stress changes in the B-Neath.

Plastic zones predicted by UTAH2 when the reduced values of material property were used are shown in Figure 10. The reduced values (Table III) account for discontinuities in the rockmass and weaker cemented backfill that result from separation of the aggregate during

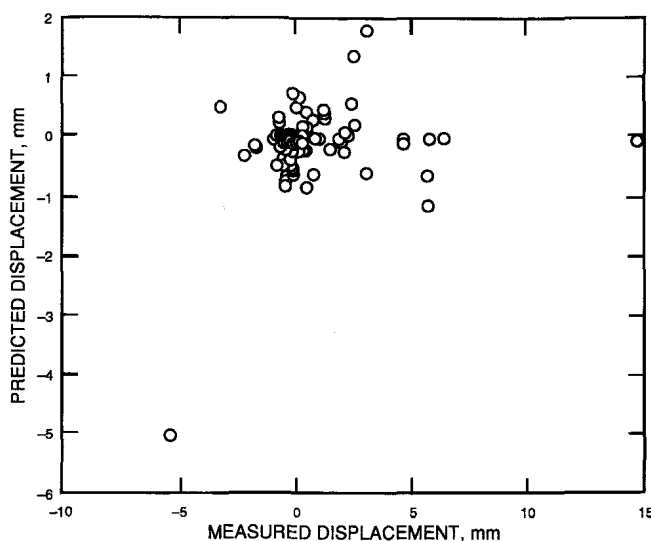


Figure 9. Measured versus predicted displacements for rock extensometers

placement. The reduced compressive strength of the silicified sandstone was calculated by use of an equation proposed by Hardy and Agapito:

$$\sigma_C = \sigma_L \times (V_L/V_F)^\alpha \times (S_F/S_L)^\beta,$$

where _L and _F = laboratory and field, respectively
 σ = strength
 V = volume
 S = width-to-height ratio
 α = volume reduction factor (0,10)
 β = shape effect factor (0,80).

The value for α is based on rock-quality designation values from the B-North orebody. The modulus of deformation for the silicified sandstone was reduced to the estimated value for the B-North orebody on the basis of the slope of the line formed by the plotting of measured versus predicted displacements². The material properties for the unsilicified sandstone were reduced in the same manner. Because the field modulus values for mudstone reported by Heuze¹¹ exceeded the values for reduced unsilicified sandstone, the reduced property values for mudstone were chosen to be the same as the reduced property values for unsilicified sandstone. A lower modulus was calculated for the cemented backfill from readings of backfill instruments in the B-North orebody, and the uniaxial compressive strength was obtained from large-scale laboratory tests².

The plastic zones shown in Figure 10 are the result of the computer run that modelled mining up to day 644, when all the sill cuts in the primary pillars had been completed, X80 had been entirely backfilled, and X86 had been backfilled to the 400 level. From a previous stability evaluation of X83 it was concluded that it failed at the 280 level and that the lower part of the pillar remained elastic³. This analysis was substantiated by the finite-element results, as shown in Figure 10, although part of the lower section of the pillar was predicted to be plastic also. In addition, the finite-element code predicted a plastic zone between the 280 and 360 levels in X92. Although no instruments had been installed in this pillar to substantiate failure, the north rib caved when benched, indicating that it may have been weakened by the presence of shear zones.

Table III
Reduced properties used in the numeric analysis

Material	Property*, MPa			ν^t
	E	C	I	
Silicified sandstone	6 894	8,3	1,00	0,25
Unsilicified sandstone	4 688	4,8	0,50	0,25
Andesite/rhyodacite	59 388	251,6	25,20	0,31
Mudstone	4 688	4,8	0,50	0,25
Cemented fill	794	4,1	0,80	0,30
Uncemented fill	159	4,1	0,80	0,30
Overburden	19	0,7	0,03	0,30

* E = Modulus of deformation

C = Unconfined compressive strength

I = Tensile strength

ν^t = Poisson's ratio

The numeric model did not predict stress redistribution to the cemented backfill pillars and was consistent with the readings of the backfill instruments. The stresses in the cemented backfill were equal to those generated by the weight of the material, indicating that the shear element at the interface between the rock and the cemented backfill performed realistically.

Conclusions

Readings from instruments installed in secondary rock pillars in the B-Neath orebody at the Cannon Mine suggested that secondary pillar X99 carried more stress during primary mining than the other secondary pillars. Local failure or slabbing in some secondary pillars was identified by these instruments and was consistent with plastic zones predicted by a finite-element model. The instruments in the cemented backfill pillars did not record additional stresses when pillar X99 lost its load-bearing capacity, indicating that the abutments carried the additional load.

The relative displacements predicted by a finite-element model of the B-Reef complex (Figure 1) had a correlation coefficient of 0,24 when paired with relative displacements measured in the rock pillars of the B-Neath orebody. This value was increased to 0,58 when eight apparent outlier data pairs were not used in the calculation. For the latter case, the measured relative displacements were approximately three times greater than the predicted values. The predicted and measured relative displacements for the cemented backfill had a low correlation coefficient.

General trends in load redistribution were identified by the use of a large number of instruments throughout the orebody and the grouping of different kinds of instruments at one location. This also helped to differentiate between apparent data anomalies and general mine behaviour. The identification of such trends can be important because mine operators can then take remedial measures, such as pillar destressing, to lower the stresses to safe levels.

Along with the identification of the general trends in stress redistribution, the instruments successfully monitored the mine safety. The borehole extensometers recorded displacements in the roof of haulage ways and stope sill cuts, while the stressmeters identified stress increases in pillar X99 and stress decreases in the remaining secondary pillars. Instruments in the pillars with cemented backfill confirmed that these pillars were not receiving additional load during secondary mining.

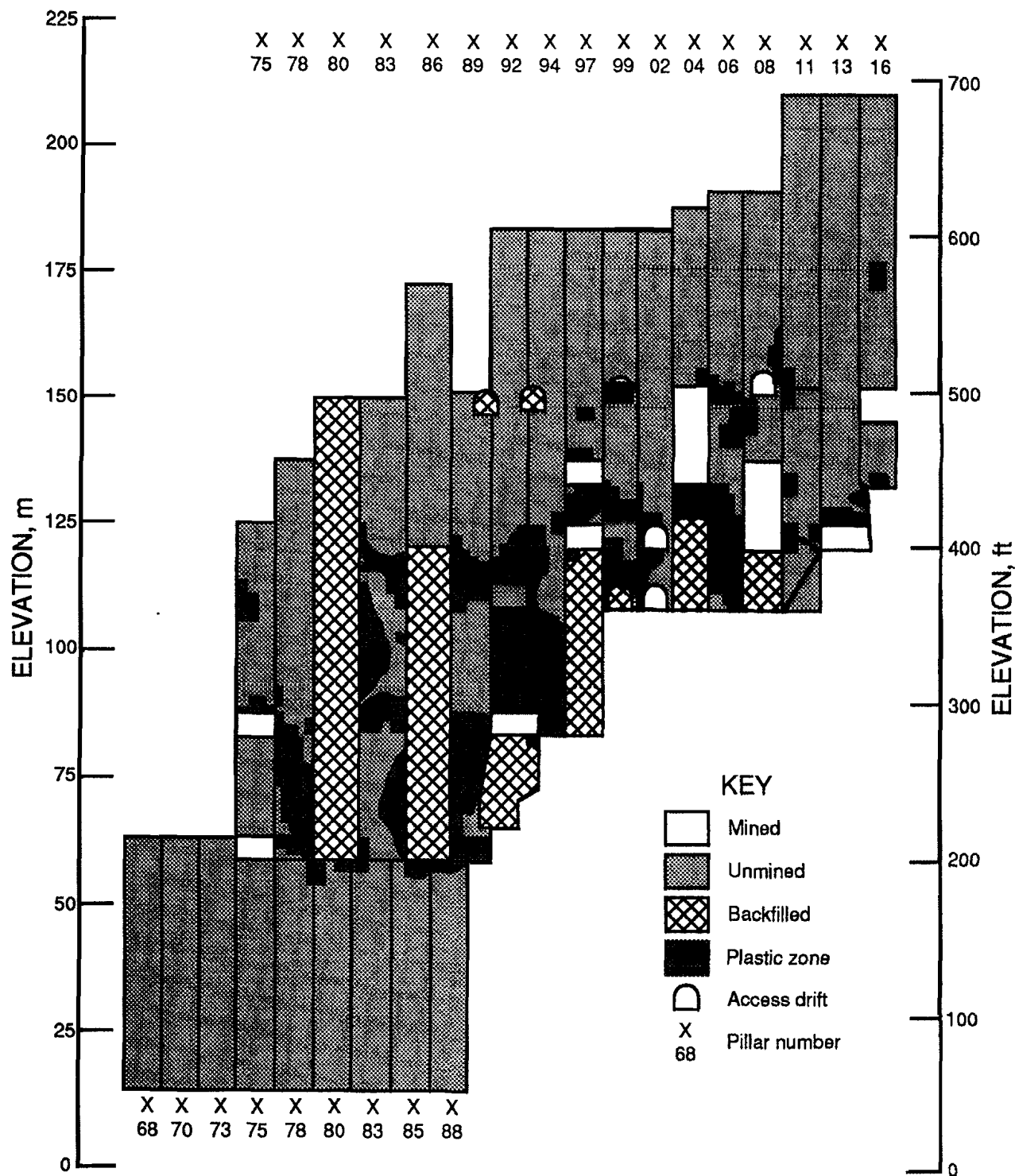


Figure 10. Plastic zones predicted by the finite-element model up to day 644

Acknowledgements

The authors thank the following personnel of Cannon Mine for providing access to the B-Neath orebody, assisting in the installation of the instruments, providing mine maps and schedules, recording instrumental data, and participating in the placement plans and purchases of the instruments: Ben Guenther, mine manager; Jim Knowlson, chief engineer; John Baz-Dresch, senior mine engineer; and Mark Fullenwider, mine engineer. The authors also thank Tony Simmonds, geotechnical engineer, Geokon, Inc., Lebanon, NH, for the early delivery of instruments when changes in installation schedules occurred and for

customizing some of the instruments; William G. Pariseau, professor, University of Utah, for interpretation of the instrumental data; and Jim Vickery, Kennecott Mining Company, for design and fabrication work on the backfill instruments.

References

- BRECHTEL, C.E., HARDY, M.P., BAZ-DRESCH, J., and KNOWLSON, J.S. Application of high-strength backfill at the Cannon Mine. *Innovations in mining backfill technology: Proceedings of the 4th international symposium on mining with backfill*.

Hassani, F.P., Scobie, M.J., and Yu, T.R. (eds.). Rotterdam, Balkema, 1989. pp. 105–117.

2. TESARIK, D.R., SEYMOUR, J.B., and VICKERY, J.D. Instrumentation and modeling of the Cannon Mine's B-North ore body. *Ibid.*, pp. 119–128.
3. BRECHTEL, C.E., AGAPITO, J.F.T., and MUDLIN, M.E. Stability evaluation during bench cut-and-fill mining of the B-Neath zone at the Cannon Mine. *Proceedings of the SME annual meeting, Las Vegas, NV, Feb. 1989.* pp. 1–16.
4. BAZ-DRESCH, J.J. Development of high productivity shotcreting at the Cannon Mine. *Mining Engineering*, Jun. 1991. p. 647.
5. PARISEAU, W.G. Interpretation of rock mechanics data: A guide to using UTAH2. (Contract HO220077, Dept. of Min. Eng., Univ. of Utah). U.S. Bureau of Mines OFR 47(2)-80, 1978. pp. 1–41.
6. DESALVO, G.J., and GORMAN, R.W. *ANSYS engineering analysis system users's manual*. Houston, Swanson Analysis Systems, Inc., 1989, vol. I, sec. 3.3. pp. 1–118.
7. FARMER, I.W. *Engineering properties of rocks*. London, Butler & Tanner, 1968. p. 37.
8. GOODMAN, R.E. *Introduction to rock mechanics*. New York, John Wiley & Sons, 1980. pp. 58, 177.
9. NICHOLSON, D.E., and BUSCH, R.A. *Earth pressure at rest and one-dimensional compression in mine hydraulic backfills*. U.S. Bureau of Mines, RI 7198, 1968. pp. 1–40.
10. SOWERS, G.F. *Introductory soil mechanics. Geotechnical engineering*. 4th ed. New York, Macmillan, 1979. pp. 180–231.
11. HEUZE, F. E. Scale effects in the determination of rock mass strength and deformability. *Rock Mechanics*, vol. 12, no. 3-4. 1980. pp. 167–192.

THE SOUTH AFRICAN INSTITUTE OF MINING AND METALLURGY

SYMPOSIUM SERIES S13

MINEFILL 93

Edited by
H.W. GLEN

THE SOUTH AFRICAN INSTITUTE OF MINING AND METALLURGY
JOHANNESBURG 1993

Contents

	<i>Page</i>
Foreword.....	xii
Committee and Sponsors.....	xiii
Values and Units Used	xiv
 SECTION 1	
Backfill Rockmass Interaction	
A Procedure for the Design of Stable Cemented Fill Exposures, M.L. Bloss, R. Cowling, and J.L. Meek	3
A Methodology for the Selection of Backfill as Local Support for Tabular Stopes in South African Gold Mines, A.P. Squelch	9
Improved Undercut-and-Fill Mining at the Garpenberg Mine, A. Fredriksson, N. Krauland, H. Stille, and S. Strömberg	17
The Assessment of Backfill Materials for Use in Tabular Stopes, A.J. Barrett and G.E. Blight	25
An Evaluation of Four Constitutive Models for the Simulation of Backfill Behaviour, A.B. Fourie, R.G. Gürtunca, G. de Swart, and E. Wendland	33
Numerical Modelling of Backfilling for Rockmass Support., M.J. Forster, W.F. Bawden, and A.J. Hyett	39
Rock-mechanics Investigations of Undercut-and-Fill Mining at the Garpenberg Mine, N. Krauland and H. Stille	47
Analysis of Backfill and Pillar Performance in the B-Neath Orebody at the Cannon Mine, D.R. Tesarik, J.B. Seymour, and M.E. Mudlin	55
Computer Modelling of the Shaft Movements Induced by the Pre-extraction and Backfilling of the Shaft-reef Area on the South Deep Mine, M.P. Raffield, J.V. James, and A.K. Isaac	65
A Finite-element Study of the Support Characteristics of Backfill, J. Yamatomi, G. Mogi, and U. Yamaguchi	73
Concrete Strike Stabilizing Pillars in Narrow-reef, Deep-level Gold Mining, G.L. Smith and G. York	83
A Review of Rock-engineering Investigations into the Benefits of Backfilling, 1986–1992, R.G. Gürtunca and N.C. Gay	93
The Use of Cemented Rockfill at Namew Lake Mine, Manitoba, Canada, A.E. Reschke	101
Instrumentation to Quantify the <i>in Situ</i> Stress–Strain Behaviour of Mine Backfill, P.S. Piper, R.G. Gürtunca, and R.J. Maritz	109
<i>In Situ</i> Performance of Cemented Backfill in a Deep-level South African Gold Mine, R.G. Gürtunca, A.R. Leach, G. York, and M.L. Treloar	121
The Replacement of Two Ventilation-shaft Pillars with Backfill from a Conventional Grouting Plant, G. Priest	129
The Effect of Backfill on Seismicity and Ground Motion in a Stope, D.A. Hemp	137
The Extraction of a Steeply Dipping, Wide Gold Reef Using Cemented Backfill, A.W. Stilwell	147

SECTION 2

Backfill System Engineering

The Production of Better Backfill by the Removal of Ultrafine Material, C.J. Uys	159
The Use of Blastfurnace Slag as a Binder in Backfill, R. Uusitalo, P. Seppänen, and P. Nieminen	169
An Assessment of the Effects of Ultrafine Aggregate Components on the Properties of Mine Backfills, A.W. Lamos	173
Advances in the Particle Sizing of Backfill, A.L. Hinde	181
A Simulation Model for the Hydraulic Transportation of Backfill, A. Sellgren and Å. Sundqvist	189
The Use of Ceramic-Epoxy Composites as Linings in Backfill Piping, A.J. Buchan	195
The Prediction of the Working Life of Backfill Pipelines, N.R. Steward and A.J.S. Spearling	201
The 'Anomalous' Flow Behaviour of Highly Concentrated Full Plant Tailings Used as Backfill, A.J.C. Paterson and J.H. Lazarus	205
The Design of Backfill Pipeline-distribution Systems by Use of Computer-aided Techniques, A.J.C. Paterson and R. Cooke	209
Backfill Shaft Columns in the Gold Fields Group, P.G. van der Walt	215
Modelling of the Flow of Highly Concentrated Backfill Slurries, R. Cooke	223
Backfill Distribution Systems in Deep Tabular Mines, D. Gericke	229
A Computer Simulation Model for the Hydraulic Transportation of Backfill, L. Gündüz and S. Durucan	241
The Optimization of Mix Designs for Cemented Rockfill, D.M.R. Stone	249
The Containment of Backfill in Deep-level South African Gold Mines, A.M. Copeland	255
The Characterization of Cemented Backfills Based on Undrained Multistage Triaxial Testing, L. Gündüz and S. Durucan	263
Backfilling Communication Systems within the Gold Fields of South Africa Group, D.C.H. Thompson	269

SECTION 3

Backfill Operation

The Tailings–Aggregate Backfilling Project at South Deep Mine, A.C. Wingrove	275
The Use of Silicated Backfill in South African Gold Mines, R.M. Smart, A.J.S. Spearling, and A.T. Harrison	289
Backfilling Operations at Cooke 3 Shaft, D.S. Webbstock, M.A. Keen, and R.A. Bradley	295
Backfilling on East Driefontein from 1983 to 1993, P.J. Cowley	307
The Use of Backfilling at Doornfontein Gold Mine, 1989–1992, M.K. Jolly	317
The Development of Backfilling Techniques in German Metal Mines during the Past Decade, W. Helms	323
Cemented-rockfilling Practices at Enonkoski and Viscaria Mines, P. Seppänen and K.-E. Marttala	333
Tests on Paste Fill at INCO, W. Lidkea and D. Landriault	337
Backfill Mining in the Yanahara Lower Orebody, Japan, U. Yamaguchi and T. Nishida	349
Mining with Cemented Backfill in the Republic of Slovenia, U. Bajželj, J. Likar, and F. Žigman	357
Backfill Research in Canada, J.E. Udd and A. Annor	361
Backfilling Operations at Mount Isa Mines 1989–1992, A.G. Grice, A. McIlwain, and K. Urquhart	369
Overview and Cost Models of Backfilling in Quebec Mines, F.P. Hassani, D. Bois, and P. Newman	375
The Backfilling Research Being Conducted by the U.S. Bureau of Mines, C.M.K. Boldt, L.A. Atkins, and F.M. Jones	389
Backfilling in an Integrated Operation Involving Coal Mining and Power Generation, F. Runovc and U. Bajželj	397
The Use of Fly Ash, Tailings, Rock, and Binding Agents as Consolidated Backfill for Coal Mines, J. Palarski	403